Plasma Science and Technology

PAPER

Discharge characteristics and reactive species production of unipolar and bipolar nanosecond pulsed gas–liquid discharge generated in atmospheric N_2

To cite this article: Jianping LIANG *et al* 2021 *Plasma Sci. Technol.* **23** 095405

Plasma Sci. Technol. **23** (2021) 095405 (12pp) https://doi.org/10.1088/2058-6272/ac132e

Discharge characteristics and reactive species production of unipolar and bipolar nanosecond pulsed gas–liquid discharge generated in atmospheric N_2

Jianping LIANG (梁建平), Xiongfeng ZHOU (周雄峰), Zilu ZHAO (赵紫璐), Hao YUAN (袁皓), Hongli WANG (王红丽), Wenchun WANG (王文春)* and Dezheng YANG (杨德正)*

Key Lab of Materials Modification (Dalian University of Technology), Ministry of Education, Dalian 116024, People's Republic of China

E-mail: wangwenc@dlut.edu.cn and yangdz@dlut.edu.cn

Received 19 April 2021, revised 10 July 2021
Accepted for publication 11 July 2021
Published 19 August 2021

Abstract

In this paper, unipolar pulse (including positive pulse and negative pulse) and bipolar pulse voltage are employed to generate diffuse gas–liquid discharge in atmospheric N_2 with a trumpet-shaped quartz tube. The current–voltage waveforms, optical emission spectra of excited state active species, FTIR spectra of exhaust gas components, plasma gas temperature, and aqueous H_2O_2, NO_2^-, and NO_3^- production are compared in three pulse modes, meanwhile, the effects of pulse peak voltage and gas flow rate on the production of reactive species are studied. The results show that two obvious discharges occur in each voltage pulse in unipolar pulse driven discharge, differently, in bipolar pulse driven discharge, only one main discharge appears in a single voltage pulse time. The intensities of active species (OH(A), and O(3p)) in all three pulsed discharge increase with the rise of pulse peak voltage and have the highest value at 200 ml min^{-1} of gas flow rate. The absorbance intensities of NO_2 and N_2O increase with the increase of pulse peak voltage and decrease with the increase of gas flow rate. Under the same discharge conditions, the bipolar pulse driven discharge shows lower breakdown voltage, and higher intensities of excited species (N_2(C), OH(A), and O(3p)), nitrogen oxides (NO_2, NO, and N_2O), and higher production of aqueous H_2O_2, NO_2^-, and NO_3^- compared with both unipolar positive and negative discharges.

Keywords: nanosecond pulse discharge, gas–liquid discharge, optical emission spectra, reactive species, FTIR spectra

(Some figures may appear in colour only in the online journal)

1. Introduction

Recently, nanosecond pulsed gas–liquid discharge (NPG-LD) with dielectric-free electrode configuration in atmospheric pressure has been widely used in many applications, including sterilization [1], water purification [2–4], biomedicine [5], and material treatment [6]. Compared with the sinusoidal discharge, the discharges driven by nanosecond pulse power supply are prone to cause lower heat and higher energy efficiency for producing reactive species [7–9]. For example, Xu *et al* have reported that the pulsed plasma jet induces higher concentrations of the aqueous H_2O_2, OH/O_2^-, $O_2^-/ONOO^-$ and has stronger bacterial inactivation compared with sinusoidal plasma jet under the same discharge power [9]. Neretti *et al* also found that the gas–liquid discharge (G-LD) generated by nanosecond pulse power is more

* Authors to whom any correspondence should be addressed.

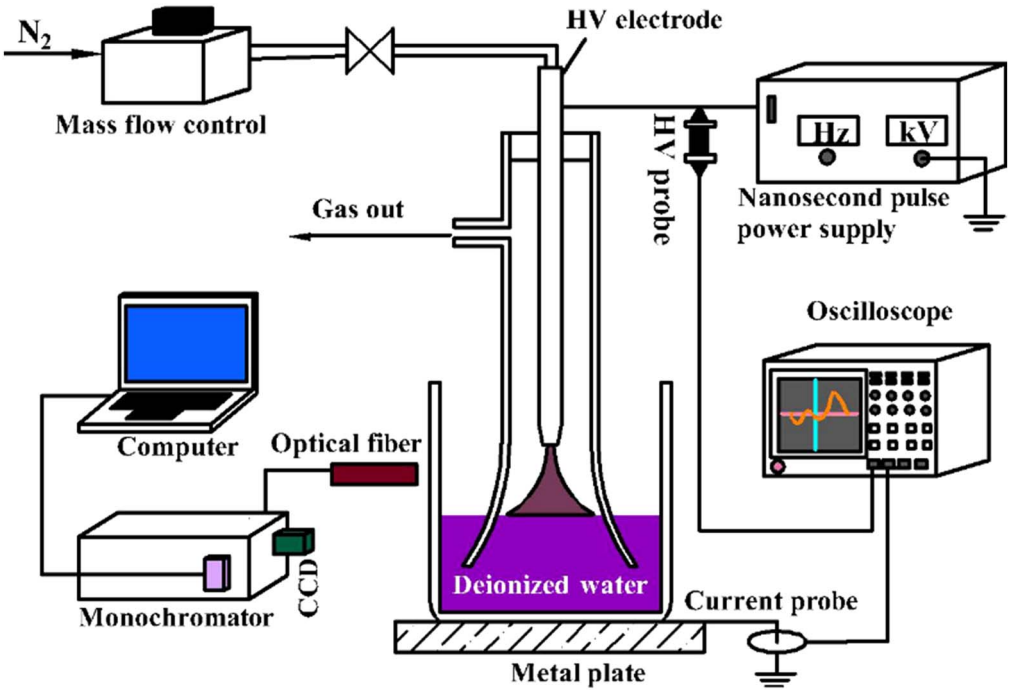

Figure 1. The experimental setup of NPG-LD.

homogeneous, has lower gas temperature, and can produce higher concentration of H_2O_2 under the same discharge power [10]. The nanosecond pulse voltage characterized by the rapid rising and falling time (∼5–50 ns) can preclude the liquid deformation caused by surface charge accumulation, and by short pulse duration time (∼10–100 ns) can avoid the undesired spark discharge [10, 11].

Many researches have used nanosecond pulse power supply to obtain G-LD with a spatial homogeneity and efficient production of reactive species at atmospheric pressure [12, 13]. It has been found that the efficiency of reactive species production and water treatment depends on the pulse polarity when NPG-LD is excited by unipolar pulse. Thagard *et al* [14] found that in the unipolar positive pulsed discharge, the production of H_2O_2 relies on the solution pH, whereas in the unipolar negative pulsed discharge, the production of H_2O_2 is lower and depends on the liquid conductivity. Hamdan *et al* [15] found that the change of the solution conductivity and pH, and concentrations of H_2O_2, NO_3^-, and NO_2^- are similar in both positive and negative polarity pulsed discharges. However, negative pulsed discharge has higher degradation rate of methylene blue, which is attributed to that the untreated solution at bottom can flow to the plasma–liquid interface at higher flow rate in negative pulsed discharge.

In recent years, bipolar pulse voltage, characterized by a negative pulse following a positive pulse alternatingly, has also been used to obtain NPG-LD. For example, Tang *et al* [16] used bipolar pulsed DBD for regenerating granular activated carbon to degrade phenol in water, and they found that phenol degradation efficiency can achieve 87% after 100 min of treatment and regeneration efficiencies of the granular activated carbon is increased with enhancing plasma treatment time. Our group also used a bipolar nanosecond pulse power to generate a stable bubble gas discharge in water, in which the H_2O_2 energy yield with Ar bubble reaches 3.04 g kW h^{-1} [17]. Although different pulse voltage modes are widely used to generate G-LD in atmosphere pressure, it has been rarely reported to compare the effects among these three pulse voltage modes on the excitation of G-LD.

Currently, obtaining a stable G-LD plasma source with large plasma volume and large plasma–liquid interface is an important challenge from the requirement of technological point. In this study, based on the typical needle-water discharge structure, a self-designed trumpet tube is added in the discharge reactor. On one hand, the addition of trumpet tube avoids the interference effect of ambient air on discharge. On the other hand, the shape of trumpet tube is beneficial for increasing the plasma source volume. According to previous discussion, the mode of nanosecond pulse supply greatly influences on the discharge properties. To optimize the discharge device, the effects of pulse mode, including unipolar negative pulse voltage, unipolar positive pulse voltage, and bipolar pulse voltage, on the discharge properties and production efficiency of active species of NPG-LD are systematically compared. The comparative studies about the plasma characteristic including electrical behavior and plasma gas temperature in three NPG-LD modes are carried. By using optical emission spectra (OES) and FTIR spectra, the effects of pulse voltage modes, gas flow rate, and pulse peak voltage on spectra intensities of gaseous reactive component are investigated. The solution pH value, and concentration of aqueous reactive species (H_2O_2, NO_2^-, and NO_3^-) are measured to discuss the different water activation mechanisms in three pulsed mode NPG-LDs.

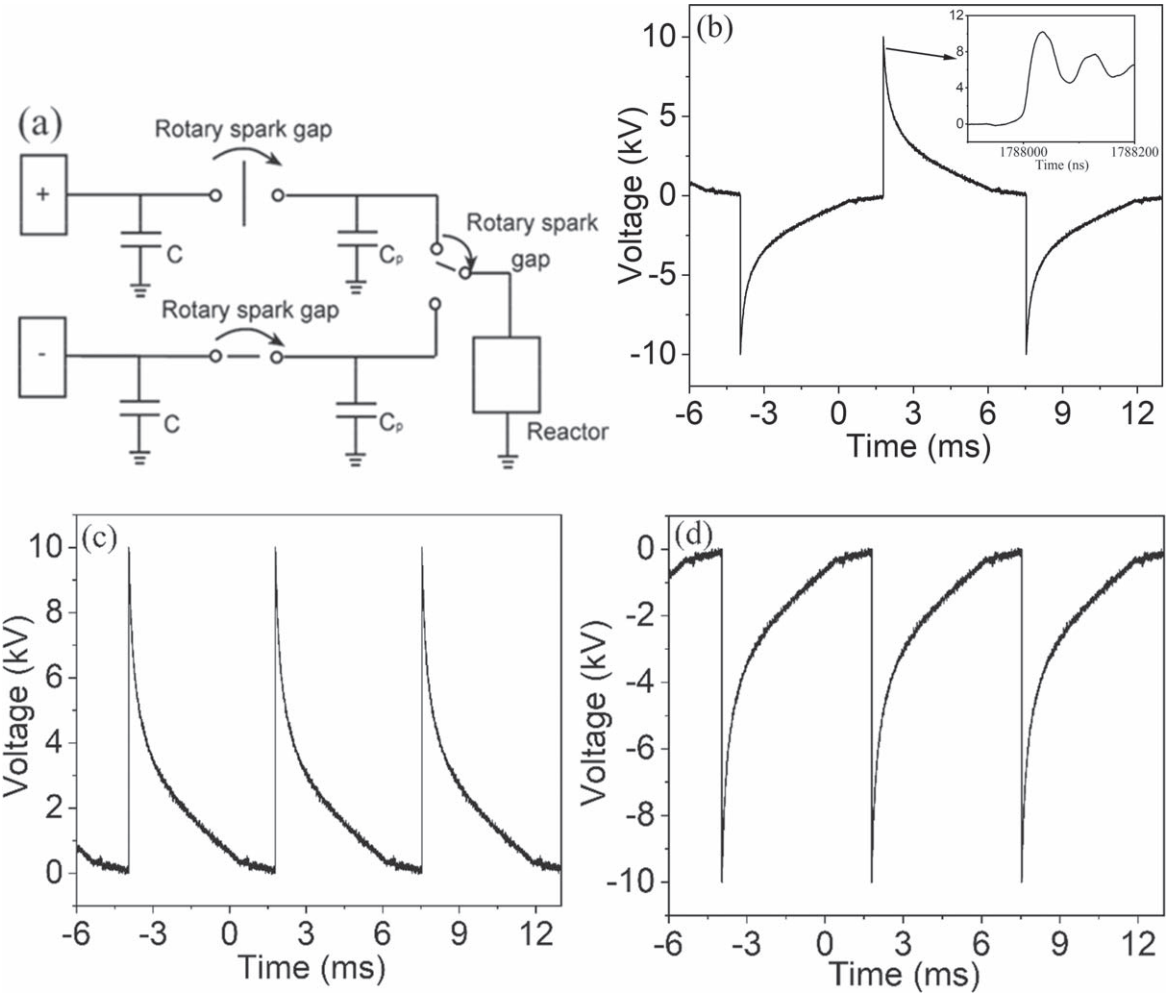

Figure 2. (a) The schematic diagram of the pulsed power supply circuit. Examples of resulting waveforms of (b) bipolar pulse, (c) unipolar positive, and (d) unipolar negative pulse voltage.

2. Experimental setup

Figure 1 shows the experimental setup, which is similar with our previous study [18]. For the discharge reactor, a trumpet quartz tube is penetrated into a quartz cup (the 25 mm inner diameter and 2 mm thickness) filled with 10 ml deionized water and fixed on a grounded metal electrode. The largest and smallest dimeters of trumpet quartz tube are 5 mm and 25 mm, respectively, and the height of the conical part is 10 mm. A high-voltage (HV) copper tube electrode (2 mm inner diameter, 3 mm outer diameter, and the smaller diameter of conic part of HV electrode is 1.5 mm) is fixed on the axial direction of a trumpet quartz tube and distances 4 mm from the liquid surface. The pure N_2 is controlled by a mass flow controller, and enters into discharge reactor through the HV electrode and flows out from the branch tube of the quartz tube. Before each discharge, the working gas pre-feds for 5 min to remove the air in the tube.

The schematic diagram of the nanosecond pulse power supply circuit is shown in figure 2(a), which has two types: positive pulse circuits and negative pulse circuits. Each circuit consists of a rotary spark gap switch, a pulsed capacitor (C_p), and a storage capacitor (C), and the C_p is used as the charged storage capacitor. Spark gap is an effective way of producing both fast rise and fall times of HV signals. The single-phase AC 220 V input is boosted by a HV transformer and then rectified to obtain a positive and negative output dc high-voltage. The dc high-voltage charges the energy storage capacitor (C) through the rotary spark gap switch to charge the pulse capacitor (C_p), and then discharges to the load through the rotary spark gap switch, so that the load obtains a high pulse voltage. When both positive and negative circuits are connected at the same time, a bipolar pulse voltage (shown in figure 2(b)) can be exported to discharge reactor. At this case, the switches of the positive and negative pulse circuits are not turned on at the same time. When positive or negative circuits are individually connected to power, the unipolar positive or negative pulse voltage can be exported to discharge reactor (shown in figures 2(c) or (d)), respectively. The pulse frequency is adjusted by changing speed of the rotary spark gap. In order to maintain the same number of pulses, 150 Hz of pulse repetition rate is used in both unipolar positive and negative pulsed modes and 75 Hz of pulse repetition rate is used in bipolar pulsed mode. The discharge images of three pulsed mode discharges are shown in figure 3, and captured by Cannon 70D digital camera with the 100 ms

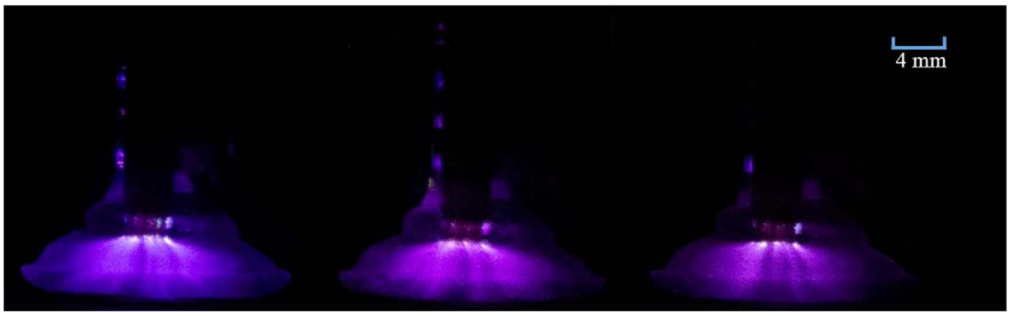

Figure 3. Images of (a) bipolar, (b) unipolar positive, and (c) unipolar negative NPG-LD under conditions of 200 ml min^{-1} gas flow rate and 30 kV pulse peak voltage.

of exposure time. The discharges in all three pulsed modes have the strongest intensity near the tips of the copper pipe, and then spread to liquid surface and fill the lower part of the trumpet quartz tube with a diffuse morphology. The discharge current and pulse voltage are measured by using an oscilloscope (Tektronix, Portland, OR, TDS5054B, 500 MHz) with a current probe (Tektronix TCP312, 100 MHz) and a 1:1000 HV probe (Tektronix P6015A, 100 MHz), respectively.

The head of the optical fiber is placed vertically to the axis of the quartz tube under all discharge conditions. The OES of plasma region is diagnosed by using a spectrometer (Andor SR750i, Andor technology, UK; sensitivity range 180–1000 nm, 1200 g mm^{-1} grating blazed at 500 nm, 0.02 nm entrance slit) equipped with a CCD camera (Newton DU940P-BV, 2048 × 512 pixels, 500 ms exposure time). The exhaust gas components of discharge reactor are analyzed by FTIR spectroscopy (Nico-LET iS10; Thermo scientific, Madison, WI) through guiding exhaust gas into absorption pool with an absorption length of 2.4 m [18]. In order to eliminate the interference of water, the anhydrous $CaCl_2$ was selected as the desiccant to remove the water in the exhaust gas before analysis. After each discharge treatment, the liquid pH is immediately detected by a pH meter (Sartorius, PB-10, Germany). The aqueous H_2O_2 concentration is measured by the titanium sulfate spectrometric method. The concentration of NO_2^- is quantified by the Griess–Saltzman method, and the concentration of NO_3^- is quantified by the 2,6-dimenthylephenol spectrometric method. All detailed measurement information of H_2O_2, NO_2^-, and NO_3^- can be found in the previous works [18, 19].

3. Results and discussion

3.1. Electrical characteristics of the NPG-LDs excited by unipolar and bipolar modes

Figures 4(a) and (b) show the waveforms of pulse voltage U and discharge current I of unipolar positive and unipolar negative NPG-LD, respectively. Figures 4(c) and (d) show pulse voltage U and discharge current I waveforms of bipolar positive pulse and negative pulse of bipolar NPG-LD, respectively. The experimental conditions are 200 ml min^{-1} gas flow rate and 30 kV pulse peak voltage. As shown in figures 4(a) and (b), the discharge current waveforms of unipolar positive and unipolar negative NPG-LDs have the similar shape except the opposite polarity. Two main discharge current peaks appear in both pulse voltage rising time and falling time of each pulse voltage. The maximum peak currents for both unipolar positive and negative NPG-LD are both about 3 A. When bipolar pulse voltage is used, it can be found that the breakdown process in bipolar pulsed discharge is completely different. According to figures 4(c) and (d), only one main discharge current peak appeared in a single voltage pulse time. Also, the maximum peak current (6 A) is much higher. Besides, it is found that the breakdown voltages in unipolar positive and negative NPG-LD are about 21 kV, while the breakdown voltage in bipolar NPG-LD is about 19 kV.

The different current waveforms and breakdown voltages between unipolar and bipolar pulse modes are related to the different discharge processes. When discharge is driven by both unipolar positive and negative pulse voltage, two main discharge current peaks appear in each pulse, which suggests that two discharges occur per pulse voltage. The similar behaviors have been found in other works which reported that the second current peak is caused by charge accumulation on dielectric surface in the first discharge [12, 20–22]. In this study, it should be noted that the quartz tube in discharge reactor is inserted into water, which is indirectly contacted with grounded electrode. In the first discharge, some charge particles can accumulate on the quartz surface. The second discharge current would be generated when potential difference between the discharge electrode and charged quartz surface is sufficient. While the charged particles accumulated on surface of quartz tube can induce opposite electric field, which results in the decrease of the electrical field intensity during the discharge period [22]. As for bipolar pulse, only one main discharge current peak in a single pulse suggests that one discharge occurred per pulse voltage. This phenomenon of the secondary discharge disappearing per pulse voltage in bipolar pulsed discharge is consistent with previously reported researches [16, 23]. As for bipolar pulse voltage, it is a negative polarity pulse followed by a positive polarity pulse alternately. During bipolar pulsed discharge process, the charges in previous pulse voltage accumulate on quartz tube surface. When voltage polarity changes, the direction of electric field caused by charges in previous pulse

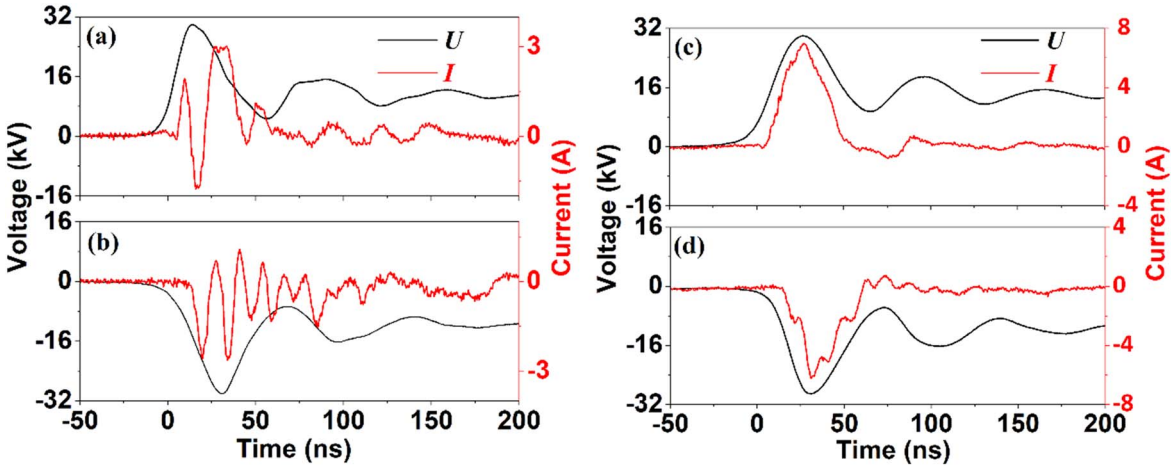

Figure 4. Pulse voltage U and discharge current I waveforms of unipolar (a) positive pulse and (b) negative pulse discharge, and bipolar pulse discharge in (c) positive pulse and (d) negative pulse.

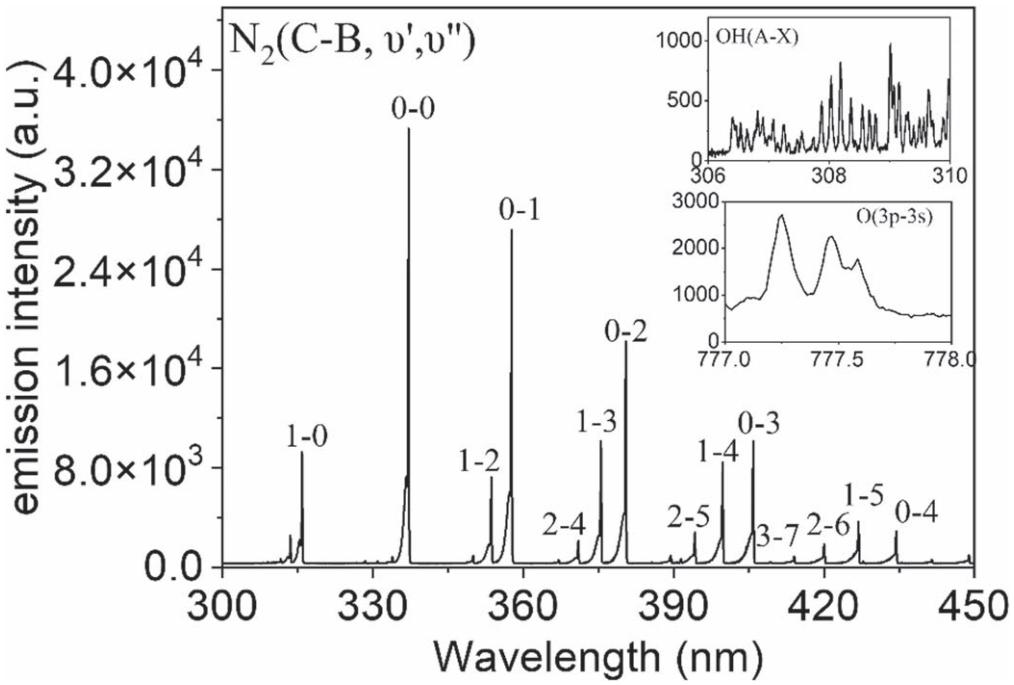

Figure 5. The OES in the ranges of 300–450 nm and 777–778 nm for bipolar NPG-LD.

is the same as the electric field generated by following pulse, and hence it results in stronger electric field and lower breakdown voltage.

3.2. OES characteristic of the NPG-LDs

Gaseous active species have the important influences on the generation of secondary aqueous active species and strongly affect water treatment efficiency [24]. Figure 5 presents the OES in the ranges of 300–450 nm and 777–778 nm for bipolar NPG-LD under 30 kV pulse peak voltage and 200 min l^{-1} gas flow rate. The OES in both unipolar positive and negative discharges (not shown) are similar with those of bipolar discharge; the detailed comparison is given in the later. As shown in figure 5, the second positive bands N_2(C–B) are the dominated, and relatively weak spectra lines including OH(A–X) and O(3p–3s, 777 nm) are also identified.

Figures 6(a)–(c) show emission intensities of N_2(C–B), OH(A–X), and O(777 nm) of unipolar (both positive and negative pulses) and bipolar discharges varied as a function of pulse peak voltage, respectively, under the condition of 100 ml min^{-1} gas flow rate. The OES reflect the transition between two states of active species, thus the OES intensity could be used to represent the relative concentration of active species for a qualitative analysis [25, 26]. In figures 6(a)–(c), the intensities of N_2(C–B), OH(A–X), and O(3p–3s) in all three pulsed discharges rise as pulse peak voltage increased, indicating that higher pulse peak voltage, the more excited states N_2(C), OH(A), and O(3p). As for those species, the excited states of OH(A), N_2(C), and O(3p) are mainly formed

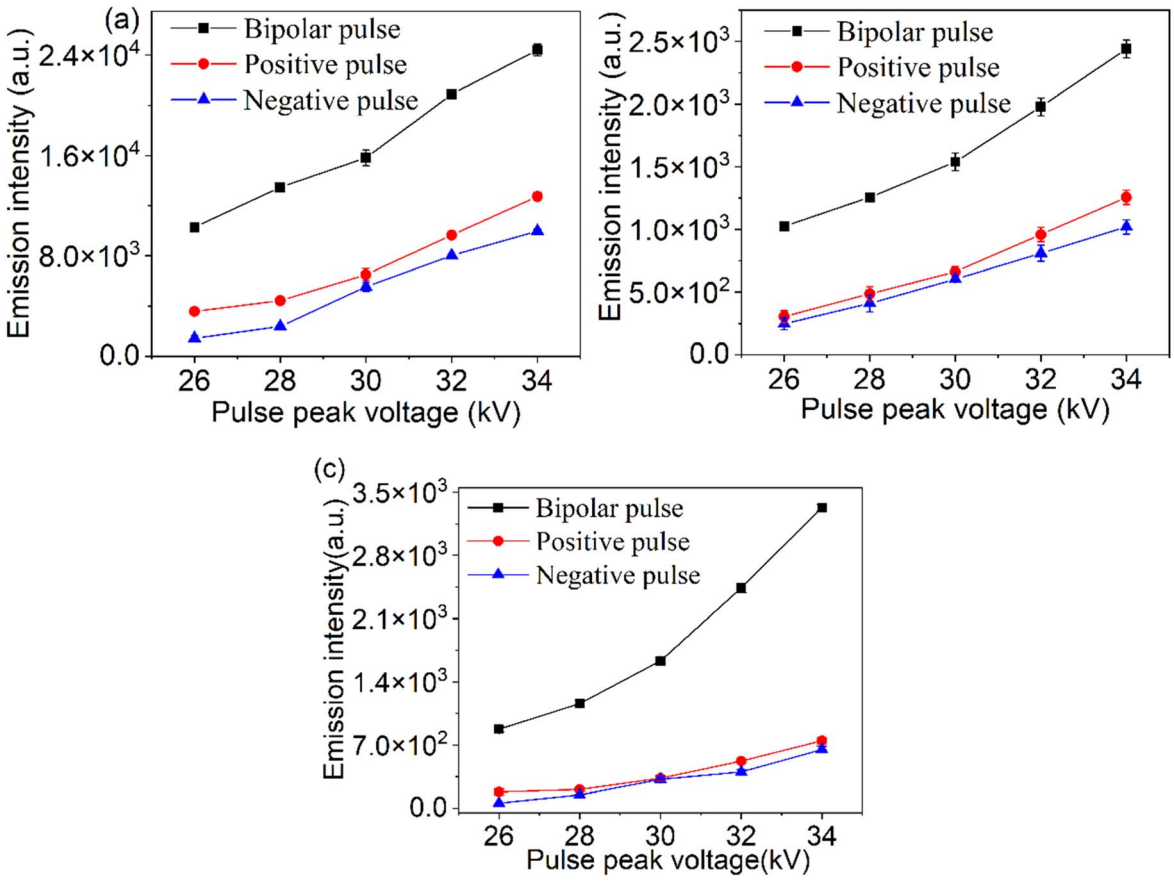

Figure 6. Effects of pulse peak voltage on the emission intensities of (a) N_2(C–B, 337 nm), (b) OH(A–X, 309 nm) and (c) O(3p–3s, 777 nm).

by the collision of energetic electron with H_2O molecules (R1), N_2 (R2), and O_2 molecules (R3), respectively. Higher pulse voltage provides more energy for the reactor, improves the average strength of the electrical field and electron density, and increases higher productions of OH(A), N_2(C), and O(3p) [26]

$$e + H_2O \rightarrow OH(A) + H + e, \quad (R1)$$

$$e + N_2 \rightarrow N_2(C) + e, \quad (R2)$$

$$e + O_2 \rightarrow O + O(3p) + e. \quad (R3)$$

Figures 7(a)–(c) shows the emission intensities of N_2(C–B, 337 nm), OH(A–X, 309 nm), and O(3p–3s, 777 nm) of unipolar (both positive and negative pulses) and bipolar discharges varied as a function of gas flow rate, respectively, under the condition of 30 kV pulse peak voltage. As shown in figure 7(a), the emission intensities of N_2(C–B) in all three pulse mode discharges decrease with rising gas flow rates. However, in figures 7(b) and (c), the emission intensities of OH(A–X, 309 nm) and O(3p–3s, 777 nm) enhance firstly with rising the gas flow rate from 100 to 200 ml min^{-1}, and then decrease when gas flow rate exceeds 200 ml min^{-1}. The weaker emission intensities of N_2(C–B) caused by higher gas flow are also found in atmospheric pressure dielectric barrier discharge reported by Zhou *et al* [27]. It should be noted that the plasma is generated in a confined quartz tube in this study, the turbulence can be formed in the tube by the gas. Li *et al* [28] investigated the effects of gas flow rate on atmosphere pressure plasma confined in a dielectric tube. They reported that faster gas flow velocity results in more charge losses due to turbulence transport of charges to the wall, which would reduce the accumulation of molecules active. Therefore, the decrease of N_2(C–B) is caused by more losses of charges at faster N_2 gas flow rate, which decreases the production of N_2(C) via (R2). Besides, rising gas flow rate leads to the increased flow of turbulences in the quartz tube, which can bring more water molecules from liquid surface to the discharge region. The dissociation energy of H_2O is about 5 eV, which is less than the excited N_2(C) (10 eV) and N_2(A) (∼5.16 eV) energy. Hence, the H_2O can be dissociated by the excited state N_2 ((R4) and (R5)) [11]. When the gas flow rate increases in the small flow rate range (100–200 ml min^{-1}), increasing a little of water molecules enhances the collision between the H_2O and high-energy species (like energy electron, excited state molecule N_2^*), which leads to produce more OH(A) and O(3p) via (R4)–(R6) [29]. However, as the gas flow rate further increases, much higher content of water vapor will have a quenching effect on the discharge due to its electronegativity, which can decrease discharge intensity, and hence decrease the production of OH(A) and O(3p)

$$N_2(C) + H_2O \rightarrow OH(A) + H + N_2(X), \quad (R4)$$

$$N_2(A) + H_2O \rightarrow O + 2H + N_2(X), \quad (R5)$$

$$e + O \rightarrow O(3p). \quad (R6)$$

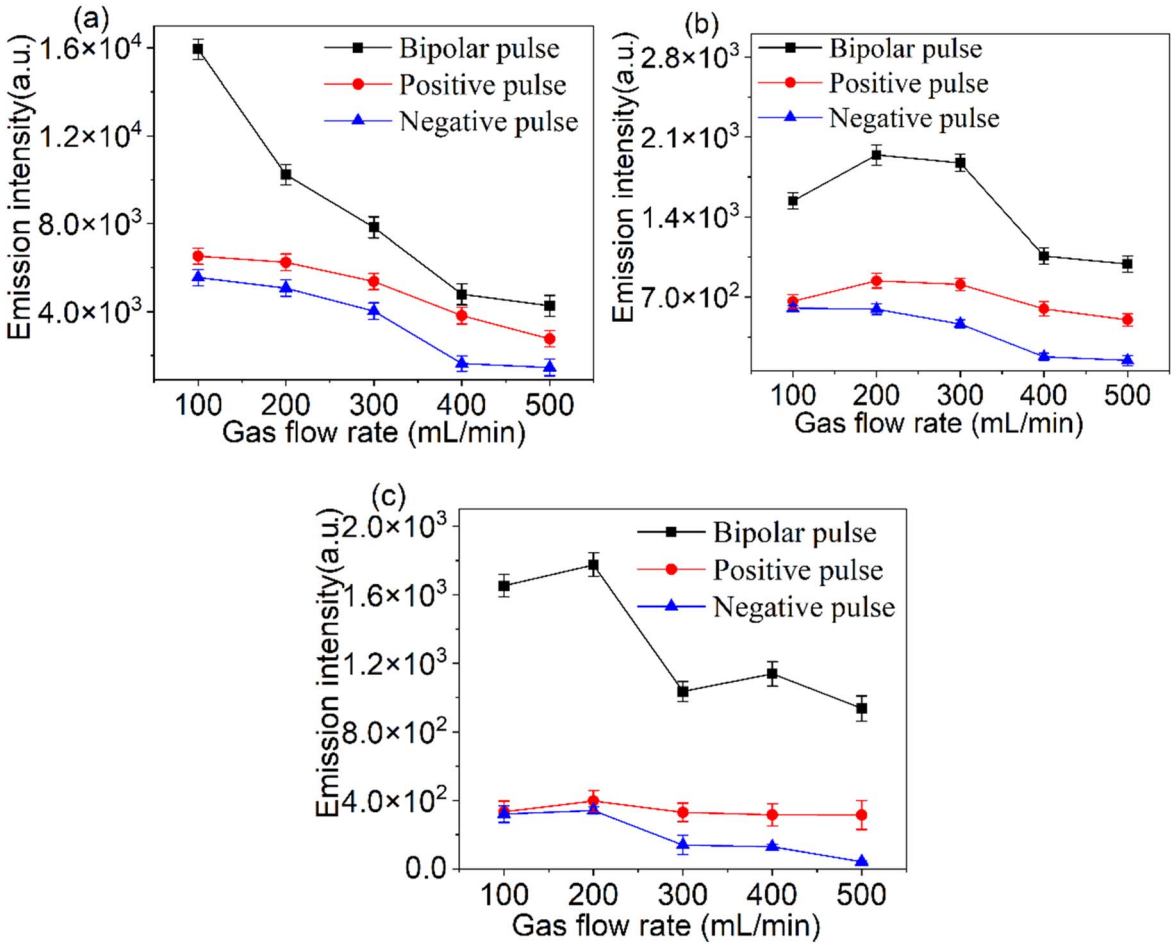

Figure 7. Effects of gas flow rate on the emission intensities of (a) N_2(C–B, 337 nm), (b) OH(A–X, 309 nm) and (c) O(3p–3s, 777 nm).

Table 1. The intensities of N_2(C–B, 337 nm), OH(A–X, 309 nm), and O(3p–3s, 777 nm) in three discharge modes.

	N_2(C–B) (a.u.)	OH(A–X) (a.u.)	O(3p–3s) (a.u.)
Unipolar negative pulse	9803.592 14	988.787 83	510.406 23
Unipolar positive pulse	10 962.474 51	1058.294 63	620.798 86
Bipolar pulse	15 816.386 85	1539.081 72	1634.083 54

In order to compare three pulse modes under the same discharge power, the 30 kV pulse peak voltage is chosen in bipolar pulse mode and 33 kV pulse peak voltage is chosen in both unipolar pulse modes. Under this condition, the power of three pulsed discharges is 0.74 W. The intensities of N_2(C–B, 337 nm), OH(A–X, 309 nm), and O(3p–3s, 777 nm) in three discharge modes are counted in table 1. It is clear that, as for the unipolar pulse mode, the polarity of pulse voltage has little effect on the excited state of active species production, and the emission intensities of those active species in unipolar positive NPG-LD are slightly higher than those in unipolar negative NPG-LD. The results are similar to the work of Hamdan *et al* [15] who reported that the concentration of gaseous reactive nitrogen and oxygen species produced by both unipolar positive and negative pulse polarities driven discharge in-contact with water is similar. However, under the same gas flow rate and pulse peak voltage, the intensities of N_2(C), OH(A), and O(3p) emitted from bipolar NPG-LD are much higher than those of unipolar (both the positive and negative) NPG-LDs. It indicates that bipolar pulse discharge is beneficial for the generation of active species. The reason is that, compared with the unipolar NPG-LD, the bipolar pulse is more efficient for delivering the energy to discharge region, and consequently increasing the electrical field strength and electron density [30]. It is confirmed by the results that the current value in bipolar NPG-LD is much higher than those in the unipolar NPG-LD (figure 4). Thus, higher electrical field and larger electron density in the bipolar NPG-LD lead to more production of OH(A), N_2(C), and O(3p).

Figure 8 shows FTIR spectra of effluent gas components of unipolar positive, unipolar negative, and bipolar NPG-LDs at 30 kV pulse peak voltage and 200 ml min^{-1} gas flow rate.

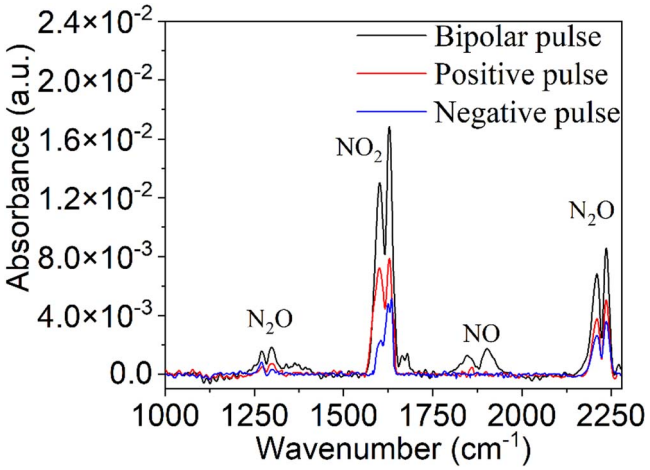

Figure 8. FTIR spectra of effluent gas components from unipolar positive pulse, unipolar negative pulse, and bipolar NPG-LD at 200 ml min^{-1} gas flow rate and 30 kV pulse peak voltage.

Table 2. The intensities of NO_2 and N_2O in three discharge modes.

	NO_2 (a.u.)	N_2O (a.u.)
Unipolar negative pulse	0.0064	0.0058
Unipolar negative pulse	0.0096	0.0069
Bipolar negative pulse	0.0168	0.0083

In both unipolar negative and positive discharges, the main products are N_2O and NO_2, almost no NO can be detected. In bipolar discharge, NO, N_2O, and NO_2 can all be detected. Also, from table 2, it is found that the absorbance intensities of both N_2O and NO_2 in bipolar pulse mode are much higher than those of both positive and negative discharges under the same discharge power. During discharge process, the nitrogen oxide (N_2O and NO) can be produced by the (R7) and (R8) [31], and the NO is easily oxidized by O and OH to form NO_2 (R9) or HNO_2 (R10) [31]. Compared with bipolar pulse mode, lower excited N_2^* and O can be produced in unipolar pulse mode (figures 6 and 7), and hence forming lower N_2O and NO_2. NO is not detected in unipolar pulsed modes, this is caused by the following reason: the production of NO formed in unipolar pulsed modes is low, and almost all NO are converted to NO_2 or HNO_2

$$N_2^* + O_2 \rightarrow N_2O + O, \quad \text{(R7)}$$

$$N_2(A) + O \rightarrow NO + N, \quad \text{(R8)}$$

$$NO + O \rightarrow NO, \quad \text{(R9)}$$

$$NO + OH \rightarrow HNO_2. \quad \text{(R10)}$$

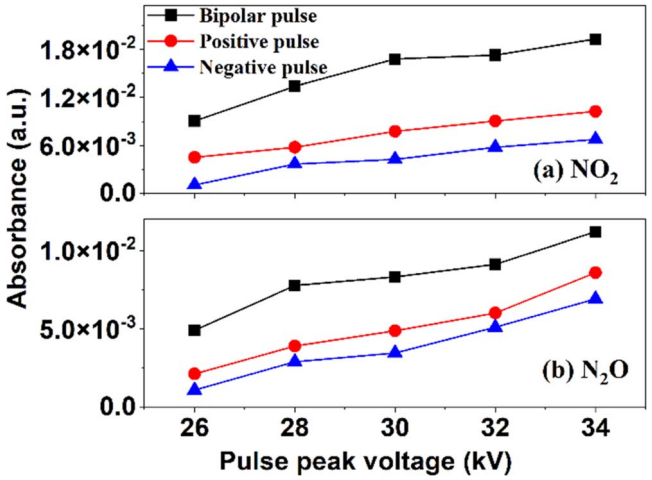

Figure 9. The effects of pulse peak voltage on the absorbance intensities of (a) NO_2 and (b) N_2O.

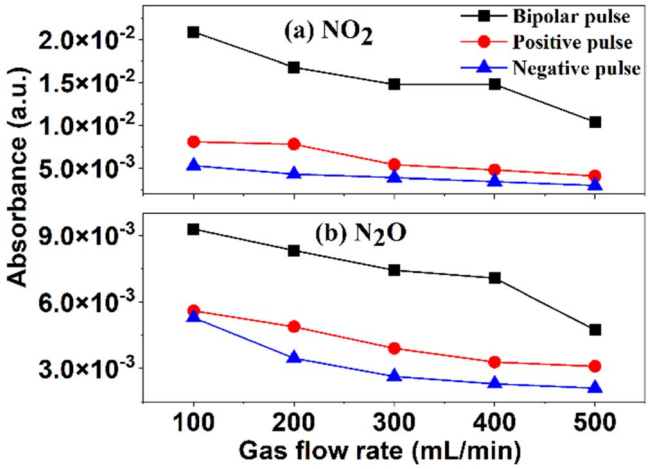

Figure 10. The effects of gas flow rate on the absorbance intensities of (a) NO_2 and (b) N_2O.

Figures 9(a) and (b) show that the absorbance intensities of N_2O and NO_2 varied as a function of pulse peak voltage, respectively, at 200 ml min^{-1} gas flow rate. It is obvious to find that the absorbance intensities of N_2O and NO_2 increase in all three pulse mode discharges when pulse peak voltage is increased, which is consistent with the change of N_2(C–B) in figure 6. In addition, figures 10(a) and (b) show that the absorbance intensities of N_2O and NO_2 varied as a function of gas flow rate, respectively, at 30 kV pulse peak voltage. It is found that the absorbance intensities of N_2O and NO_2 decrease when gas flow rate is raised in all three pulse mode discharges, which is also consistent with the change of N_2(C–B) in figure 7. Combining with the previous results, it is suggested that increasing pulse voltage and decreasing gas flow are beneficial for producing excited N_2^*, which further increase the production of nitrogen oxide.

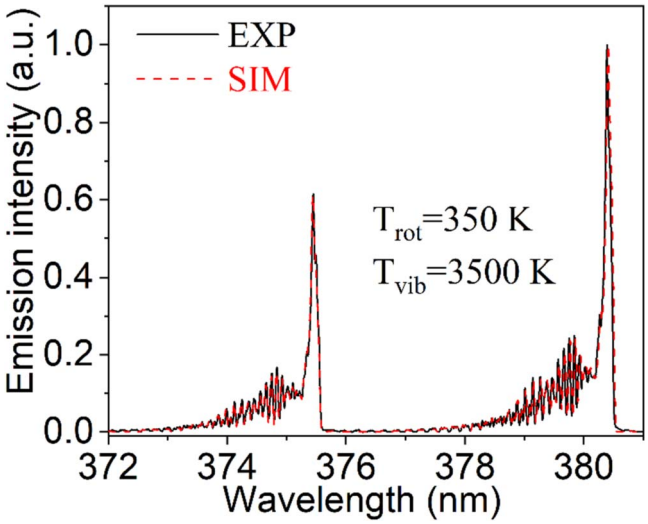

Figure 11. The experimental spectra of N_2(C–B, 0–2) and correspondingly simulated spectra under 30 kV pulse peak voltage and 200 ml min^{-1} gas flow rate.

3.3. Plasma temperature of NPG-LDs excited by unipolar and bipolar modes

The gas temperature is a very important parameter of plasma that affects the chemical reaction pathways and final products, and subsequently affects the performance of water treatment applications [32]. The rotational temperature (T_{rot}) of N_2(C) molecule is approximately equal to the gas temperature if the next two requirements are satisfied [8, 33]. First, the relaxation time (τ_{RT}) of equilibrium between translation and rotation of N_2(C) achieved via collision, is less than or equal to the lifetime (τ_0) of N_2(C) that has considered the quenched process in atmospheric pressure. Second, the excited state N_2(C) are mainly generated by the direct electron excitation of ground state N_2(X). In nanosecond pulsed discharge, the τ_{RT} is in the order of ns (1–3 ns) due to high frequent collision, which is much lower than τ_0 in the order of several ten ns [8]. Besides, N_2 gas is used as working gas, the formation processes of excited sate N_2(C) satisfy the second requirement. Therefore, in this study, the T_{rot} of N_2(C) can be approximately equal to the gas temperature. By using the SPECAIR software [34], the T_{rot} and vibrational temperature (T_{vib}) can be obtained by comparing experimental spectra of N_2(C–B, 0–2) with a best simulated spectra. Figure 11 displays the experimental spectra and simulated spectra of N_2(C–B, 0–2). As shown in figure 11, the T_{vib} and T_{rot} of N_2(C–B, 0–2) are 3500 K and 360 K in bipolar NPG-LD, respectively, under the condition of 200 ml min^{-1} gas flow rate and 30 kV pulse peak voltage. It indicates that gas temperature of bipolar pulse discharge plasma is 360 K.

The effects of pulse voltage on T_{rot} and T_{vib} of unipolar positive pulse, unipolar negative, and bipolar NPG-LDs are shown in figure 12. It is shown that in all three discharge modes, the T_{rot} always maintain at a low level. When the pulse peak voltage enhances from 26 to 34 kV, the T_{rot} in all three discharge modes only rise from 340 to 410 K. In comparison, the T_{rot} in three pulsed discharge modes have a near value under same discharge conditions. The results indicate that the NPG-LD excited by whatever pulse modes has a weak gas heating effect. In the process of nanosecond pulse discharge, the main energy delivered to discharge is preferentially used to generate high-energy electrons rather than heating the ions and gas molecules [12, 35]. In addition, since time interval between two discharges is much longer than the duration time of nanosecond pulse at the low repetition, the gas can be cooled effectively, consequently, thermal instability can be effectively suppressed. Therefore, the NPG-LDs excited by all pulse modes have relatively low gas temperature. Besides, it is found that the increased temperature of liquid treated by the discharge is less than 2 K under the all discharge conditions after 10 min discharge treatment, suggesting that the NPG-LDs have no obvious heating effect on liquid.

According to figure 12(b), the T_{vib} of NPG-LDs excited by all bipolar and unipolar pulse voltages rise with the increase of pulse voltage. Such an increase trend in T_{vib} has also been reported by Wang *et al* [36], the authors claimed that higher pulse voltage causes higher electron density, which increases frequent collisions between energy electrons and N_2 molecules. And thus, the population in high vibrational states will increase, consequently, resulting in a significant increase of the vibrational temperature. Also, T_{vib} are found much higher than T_{rot} in three pulse modes, which indicates that plasmas in all three pulsed discharges have extremely high degree of the non-equilibrium [8, 12]. In comparison, as for unipolar pulse mode, voltage polarity has no appreciable influence on T_{vib} under a certain pulse voltage. However, T_{vib} in bipolar pulse mode is about 300 K higher in bipolar pulse mode than that in unipolar pulse mode. This is because the population quenching between vibrational levels at excited electronic states is less sufficient than that of rotational levels due to bigger vibrational gaps [37]. Under the same discharge condition, the bipolar pulse mode induces more excited state N_2, which leads to higher T_{vib}, compared with both unipolar pulse modes.

3.4. Analysis of solution pH value and production of NO_3^-, NO_2^-, *and* H_2O_2

To determine the effect of pulse polarity on the different characteristics of the G-LDs in N_2, the aqueous long-lived species concentrations are measured. Figures 13(a)–(d) show that the solution pH value, and the concentrations of NO_3^-, NO_2^-, and H_2O_2 varied as a function of plasma treatment time, respectively. The experimental conditions are 30 kV pulse voltage and 200 ml min^{-1} gas flow rate. Based on figure 13(a), during the first 6 min, the pH values in both unipolar pulse modes are almost unchanged, and meanwhile in bipolar pulse mode, it rapidly decreases as plasma treatment time is increased. When the plasma treatment time exceeds 6 min, the pH value begins to decrease, and meanwhile in bipolar pulse mode, it reaches a stable value (about 3.8) which is lower than that in unipolar discharge. Besides, NO_3^- and NO_2^- in all three pulsed discharges modes show an increase trend as plasma treatment time is increased (shown in

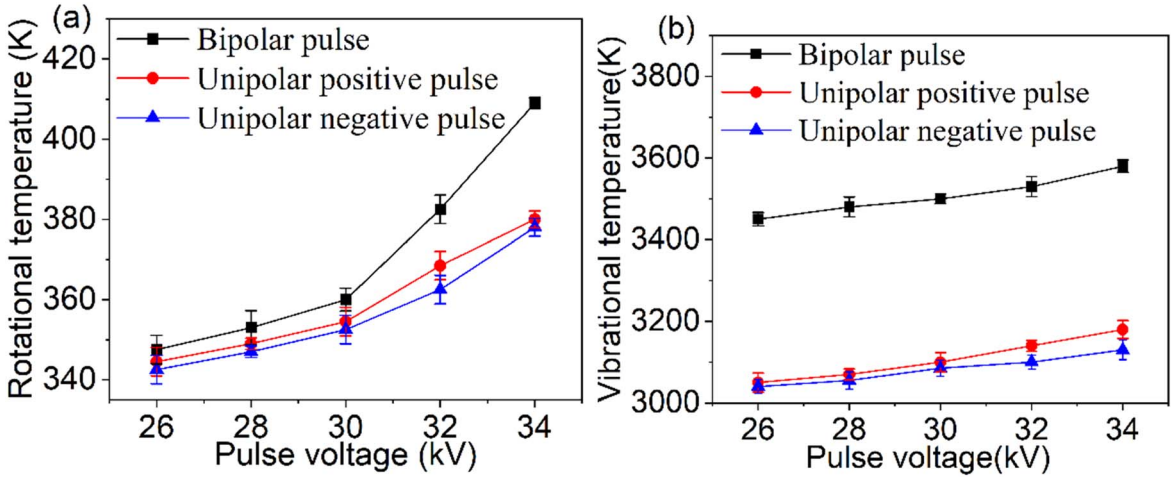

Figure 12. Effects of pulse peak voltage on (a) T_{rot} and (b) T_{vib} of NPG-LDs generated by bipolar pulse, positive pulse, and negative pulse.

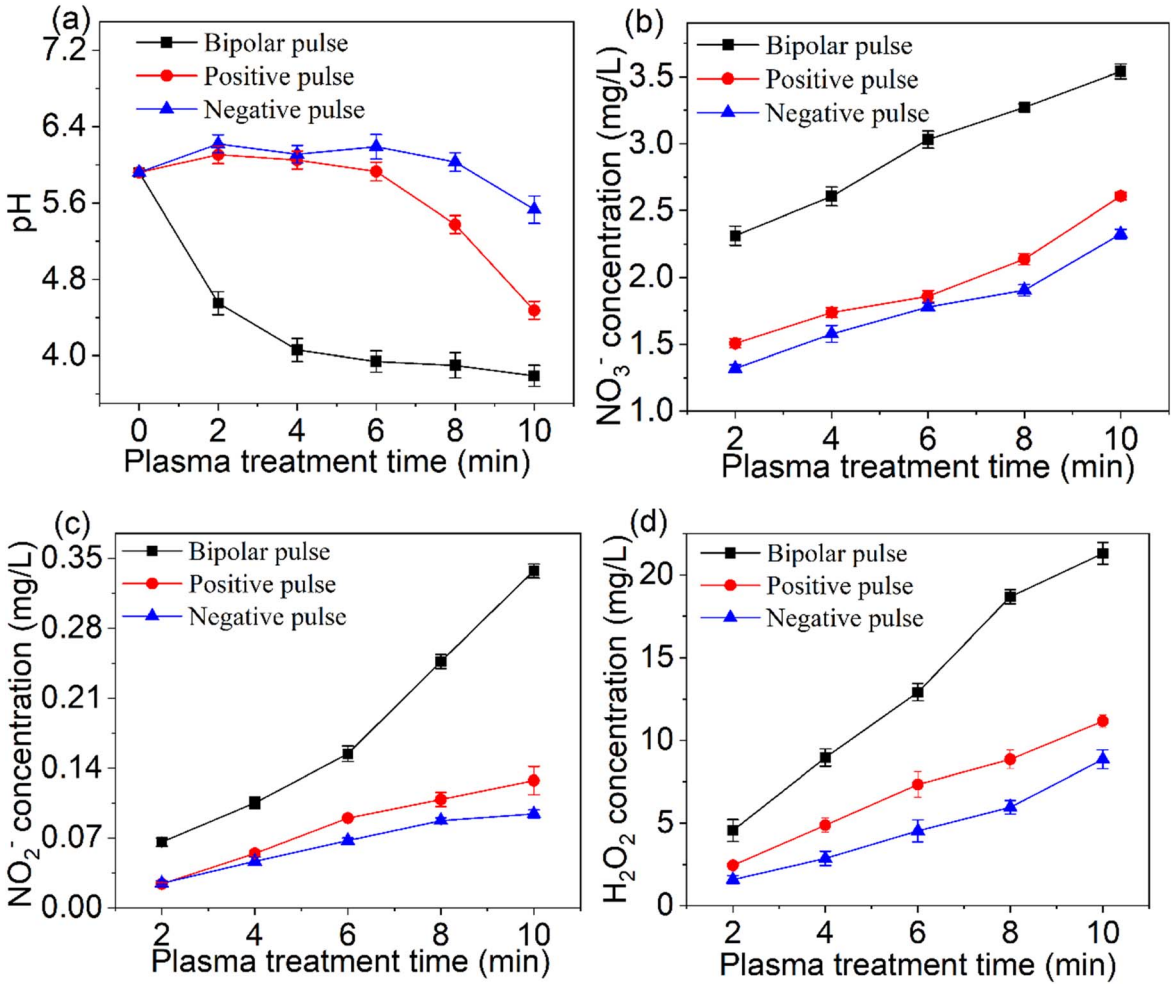

Figure 13. (a) pH of solution, (b) NO_3^-, (c) NO_2^-, and (d) H_2O_2 concentration varied as a function of plasma treatment time.

figures 13(b) and (c)). In comparison, NO_3^- and NO_2^- concentrations are close in both unipolar positive and negative pulse modes, which is consistent with the works of Hamdan *et al* [15]. While the concentrations of the reactive species in bipolar mode is much higher than those in both unipolar pulse modes. The generation of NO_2^- and NO_3^- is mainly originated from the dissolution of NO and NO_2 ($2NO_2 + H_2O \rightarrow H^+ + NO_2^- + NO_3^-$; $NO + NO_2 + H_2O \rightarrow 2H^+ + 2NO_2^-$) [24, 38, 39]. Higher contents of gaseous NO and NO_2 in bipolar pulse discharge lead to higher production of NO_2^- and NO_3^-.

Meanwhile, the formation processes of NO_x^- cause the production of H^+, and higher production of NO_x^- in bipolar pulse mode also causes lower pH value (higher production of H^+).

H_2O_2 is a major long-lived reactive species in plasma and plays an important role in plasma microbial inactivation [40]. In general, several reactions of H_2O_2 formation have been reported in interaction of plasma–liquid, however, the main pathway is the recombination of two OH radicals ($OH + OH \rightarrow H_2O_2$) [41]. According to figure 13(d), the concentrations of H_2O_2 in all pulsed discharge modes increase with increasing treatment time. After 10 min treatment time, the energy yield in unipolar positive pulse driven discharge is 1.10 g kW^{-1} h^{-1}, which is larger than those in unipolar negative pulse driven discharge (0.88 g kW^{-1} h^{-1}), the similar results are also obtained by He *et al* [42] and Chen *et al* [41]. He *et al* [42] reported that lower energy yield of H_2O_2 in the discharge driven by the negative direction voltage is due to the existence of a cathode voltage fall on the liquid surface. Chen *et al* [41] reported that discharge with liquid anode can produce more aqueous OH than that of discharge with liquid cathode, which results in higher production of H_2O_2 produced by discharge driven by the positive direction voltage. Besides, the energy yield of H_2O_2 in bipolar mode is 1.78 g kW^{-1} h^{-1}, which is much larger than those in unipolar modes. The fastest production rate of H_2O_2 in bipolar pulse mode can be basically caused by the following reasons: the production of OH is related to the charge density and discharge energy. The higher the charge density and discharge energy, the more OH are produced [43]. When the unipolar pulse voltage is used to excite discharge, charges can accumulate at the quartz tube and water surface, which decreases the electrical field and electron density. However, the bipolar pulse voltage can eliminate such charge accumulation [21]. Hence, higher charge density and discharge energy cause higher production of OH, which resulting in higher production of H_2O_2.

4. Conclusions

In this paper, a comparison of the atmosphere pressure N_2 NPG-LDs driven by unipolar (both negative and positive pulses) and bipolar pulses in a trumpet tube is experimentally studied. It can be concluded that diffuse NPG-LD can be obtained under the excitation of all three pulse modes in atmospheric N_2. The discharge process is completely different between unipolar (both positive and negative) and bipolar pulsed discharges. In both negative and positive NPG-LDs, twice discharges occur in rising time and falling time of each voltage pulse. While only one relatively strong current peak appears in a single pulse of bipolar NPG-LD. However, the gas temperatures of plasmas in three discharge modes are near and kept relative low values (340–410 K) with increasing the pulse voltage from 26 to 34 kV. Besides, rising pulse peak voltage can contribute to increase the emission intensities of OH(A–X), N_2(C–B), and O, while the emission intensities of OH(A–X) and O have the largest values at around 200 ml min^{-1}. The FTIR absorbance intensities of NO_2 and N_2O enhance with the increase of pulse peak voltage and decrease with the increase of gas flow rate.

The polarity of unipolar pulse voltage has a little effect on the discharge current and reactive species production. Compared with unipolar pulse discharge, the bipolar pulse discharge shows lower breakdown voltage and larger production rate of reactive species. Under the same discharge power, the emission intensities of OH(A–X), N_2(C–B), and O(3p–3s) in bipolar pulse discharge are higher than those in unipolar (both the positive and negative) pulse discharge. The absorbance intensities of NO_2 and N_2O are higher in bipolar pulse mode than those in both unipolar pulse modes. Solution pH value in bipolar mode is much lower, and the concentrations of H_2O_2, NO_2^-, and NO_3^- in bipolar pulse mode are much higher than those in unipolar modes (both positive and negative pulses).

Acknowledgments

This work is supported by National Natural Science Foundation of China (Nos. 51977023, 51677019, and 11965018) and Fundamental Research Funds for the Central Universities in China (No. DUT18LK42).

References

[1] Li Y *et al* 2016 *Plasma Sci. Technol.* **18** 173
[2] Liu W Z *et al* 2018 *Plasma Sci. Technol.* **20** 014003
[3] Ren J Y *et al* 2019 *Plasma Sci. Technol.* **21** 025501
[4] Zhou X F *et al* 2021 *J. Hazard. Mater.* **403** 123626
[5] Judée F *et al* 2019 *J. Phys. D: Appl. Phys.* **52** 245201
[6] Attri P *et al* 2015 *Sci. Rep.* **5** 8221
[7] Wang Q *et al* 2018 *Plasma Sci. Technol.* **20** 035404
[8] Evans M D G *et al* 2015 *J. Phys. D: Appl. Phys.* **48** 255203
[9] Xu H *et al* 2018 *Phys. Plasmas* **25** 013520
[10] Neretti G *et al* 2016 *Plasma Sources Sci. Technol.* **26** 015013
[11] Wang S *et al* 2020 *Plasma Process. Polym.* **17** 1900146
[12] Jiang N *et al* 2017 *J. Phys. D: Appl. Phys.* **50** 155206
[13] Wang S *et al* 2018 *Plasma Sci. Technol.* **20** 075404
[14] Thagard S M, Takashima K and Mizuno A 2009 *Plasma Chem. Plasma Process.* **29** 455
[15] Hamdan A *et al* 2020 *J. Phys. D: Appl. Phys.* **53** 355202
[16] Tang S F *et al* 2018 *Plasma Sci. Technol.* **20** 054013
[17] Zhou X F *et al* 2019 *Plasma Process. Polym.* **16** 1800124
[18] Liang J P *et al* 2019 *Phys. Plasmas* **26** 023521
[19] Liang J P *et al* 2020 *Vacuum* **181** 109644
[20] Xiong L *et al* 2019 *Phys. Plasmas* **26** 063511
[21] Sung T L *et al* 2013 *Vacuum* **90** 65
[22] Yuan D K *et al* 2017 *Plasma Chem. Plasma Process.* **37** 1165
[23] Guo H F *et al* 2019 *J. Appl. Phys.* **125** 163304
[24] Stancampiano A *et al* 2018 *Plasma Sources Sci. Technol.* **27** 125002
[25] Zhao Z *et al* 2018 *Plasma Sci. Technol.* **20** 115403
[26] Baek E J *et al* 2016 *Phys. Plasmas* **23** 073515
[27] Zhou S Y *et al* 2019 *J. Phys. D: Appl. Phys.* **52** 265202
[28] Li S Z, Huang W T and Wang D Z 2009 *Phys. Plasmas* **16** 093501
[29] Verreycken T and Bruggeman P J 2014 *Plasma Sources Sci. Technol.* **23** 015009
[30] Hippler R *et al* 2019 *Plasma Sources Sci. Technol.* **28** 115020
[31] Schmidt-Bleker A *et al* 2016 *Plasma Process. Polym.* **13** 1120

[32] Xi W *et al* 2020 *Plasma Sources Sci. Technol.* **29** 095013
[33] Bruggeman P J *et al* 2014 *Plasma Sources Sci. Technol.* **23** 023001
[34] Laux C O *et al* 2003 *Plasma Sources Sci. Technol.* **12** 125
[35] Wandell R J *et al* 2019 *Plasma Chem. Plasma Process.* **39** 643
[36] Wang S *et al* 2019 *J. Appl. Phys.* **125** 043304
[37] Yang F X, Mu Z X and Zhang J L 2016 *Plasma Sci. Technol.* **18** 79
[38] Abdelaziz A A, Ishijima T and Tizaoui C 2018 *J. Appl. Phys.* **124** 053302
[39] Zhou X F *et al* 2019 *Plasma Process. Polym.* **16** e1900001
[40] Kondeti V S S K *et al* 2018 *Free Radic. Biol. Med.* **124** 275
[41] Chen Z Y *et al* 2018 *J. Phys. D: Appl. Phys.* **51** 325201
[42] He B B *et al* 2017 *J. Phys. D: Appl. Phys.* **50** 445207
[43] Ono R and Tokuhiro M 2020 *Plasma Sources Sci. Technol.* **29** 035021